Lane Identification with Real Time Single Frequency Precise Point Positioning: A Kinematic Trial

R.J.P. van Bree, P.J. Buist, C.C.J.M Tiberius, *Mathematical Geodesy and Positioning (MGP),*
B. van Arem, *Transport and Planning,*
V.L. Knoop, *Delft Center for Systems and Control,*
Delft University of Technology, The Netherlands

BIOGRAPHIES

Roel J.P. van Bree graduated in Astronomy from Leiden University in the Netherlands in 1997. He has worked for ten years at TNO Defense and Security on Synthetic Aperature Radar (SAR). Currently he is working as a research associate at Delft University of Technology (DUT) on Precise Point Positioning (PPP) and navigation with GPS and Galileo.

Peter J. Buist is a GNSS researcher at DUT. He received his master degree in the field of aerospace engineering from DUT. After eight years in the Japanese industry working on GNSS applications for space, Peter returned to Delft. His research interests includes mass market applications of GNSS.

Christian C.J.M. Tiberius is an associate professor at Delft University of Technology. He is involved in GNSS positioning and navigation research since 1991, currently with emphasis on data quality control, SBAS and Precise Point Positioning.

Bart van Arem is a full professor in Transport & Planning at Delft University of Technology. He holds an MSc and PhD degree in Applied Mathematics in queuing theory, at the University of Twente, the Netherlands. He has worked at TNO on Intelligent Transport Systems for many years. His interest lies in Advanced Driver Assistance systems and on the impact of Intelligent Transport Systems on mobility.

Victor L. Knoop received his Master's degree in Physics from Leiden University in 2005, and his PhD degree from Delft University of Technology in 2009 on the effects of incidents on driving behaviour and traffic congestion. After a Post-Doc at the University of Lyon on the subject of lane changing, he is again with Delft University of Technology. His main research interest is the interaction between microscopic and macroscopic traffic flow phenomena.

ABSTRACT

The performance of real-time single frequency GPS Precise Point Positioning is demonstrated in terms of position accuracy, with the application of lane-identification for road-traffic in mind. This Precise Point Positioning technique relies on predicted satellite orbits, predicted Global Ionospheric Maps, and in particular on real-time satellite clock estimates, which are obtained from the RETICLE system of the German Space Operations Center (GSOC) / German Aerospace Center (DLR). A kinematic experiment was carried out, under true operational circumstances, with a car on the motorway between Rotterdam and The Hague in the Netherlands, employing a range of different GPS-equipment. The test demonstrates that the requirement of a 95% horizontal position component error smaller than 1.75 m for lane-identification is easily met with high-end and middle-class equipment, and most of the time also with lower end equipment (u-blox) with a patch antenna. With real-time Precise Point Positioning employing high-end and middle-class equipment, using solely single frequency measurements (on L1), 95% errors in the horizontal position components can get as low as 0.3-0.4 m.

INTRODUCTION

Lane identification on a motorway may be required for next generation car navigation, and advanced driver assistance in general, as well as to support the observation and study of driver behaviour and traffic flow. These road vehicle applications call for sub-meter positioning accuracy, and some of them even for real-time operation, and all this preferably at low-cost.

In this contribution we will investigate whether Real-Time Single Frequency Precise Point Positioning (RT SF-PPP) can meet the demands set by the above applications. Precise Point Positioning offers improved position accuracy, as compared to standalone GPS positioning, but without the need for local or regional DGPS-like infrastructure.

The best position accuracy with SF-PPP is reached when as precise as possible GPS data products are used, i.e. final satellite clocks and satellite orbits, final ionospheric maps and the latest Differential Code Biases (DCBs). These products however are available to a user with a significant latency of a few days or even weeks after the measurement epoch, ruling out real-time operation.
For real-time operation, predicted satellite orbits, predicted Global Ionospheric Maps (GIMs), and in particular real-time satellite clock estimates must be used. For the latter, the Real-time Clock Estimation (RETICLE) products from the German Space Operations Center (GSOC) / German Aerospace Center (DLR) [6] are used here, which have been shown to deliver comparable performance with IGS final products in [2].
At Delft University of Technology, a real-time version of SF-PPP has been developed. The SF-PPP algorithm uses un-differenced single frequency pseudorange code and carrier phase observations of the user receiver in the vehicle, together with the aforementioned data products. The position solution is computed on an epoch by epoch basis, truly kinematic, without (relying on) any modeling of the user receiver dynamics.
Performance of Real Time Single Frequency Precise Point Positioning was extensively demonstrated in [2] and [3] for static applications. The position accuracy presented in [3] shows, a 95% error of about 0.30 meter in the horizontal directions, and 0.65 meter in the vertical. These results were obtained using high-end GPS receivers. For middle-class receivers these values were found to be still smaller than one meter in all directions. These findings have led to the question: can SF-PPP deliver the position performance required for lane identification of a road vehicle, in real-time, and preferably with low-cost equipment? Low-cost refers here to a fairly simple single frequency GPS receiver, with a patch antenna, delivering pseudorange code and carrier phase observations, with a cost on the order of 100 Euro or less.

Figure 1: Testing took place on the busy A13 multi-lane motorway, between the cities of Rotterdam and The Hague in the Netherlands, also during early morning rush-hour (6 o'clock local time), in measurement session 3.

This research question is answered by a kinematic trial performed with a vehicle on the road, recently, in Spring 2011. The multi-lane motorway (A13) used for the test is located between the cities of The Hague and Rotterdam, runs along Delft, and is one of the busiest motorways in the Netherlands. The test was carried out under ordinary driving conditions. The purpose of the trial was to assess the position accuracy and to test specifically the ability to identify the lane the car is driving in.
For the test the antennas of low-end and middle-class receivers were all rigidly mounted on the test vehicle´s roof, next to several antennas of high-end equipment. The latter are used to reconstruct an accurate (cm-level) ground-truth for the low-end and middle-class receivers, using (dual frequency) differential carrier-phase GPS to a nearby reference station, namely a permanent GNSS station at TU Delft´s GNSS observatory, with accurately known position coordinates in the International Terrestrial Reference Frame (ITRF2005). In this way a highly accurate reference track is available for quantitative error analysis of the obtained PPP-results.
In this paper we will first provide a brief introduction to Single Frequency Precise Point Positioning, next, describe the application and outline the requirements for lane-identification, describe the test set-up, and then present and discuss the results.

PRECISE POINT POSITIONING

At present SF-PPP is already used in the GNSS community. A detailed description of SF-PPP can be found in [7], [13], [5] and [10]. The best position accuracy with SF-PPP is reached when as precise as possible GNSS data products are used, i.e. final satellite clocks and orbits, final ionospheric maps and the latest Differential Code Biases (DCB). These products however are available to the user with a significant latency of a few days or even weeks after the measurement epoch. When a real-time position solution is requested, *predicted* satellite clocks, orbits and ionospheric maps must be used, resulting in a position solution with a much larger error.
Instead of using predicted ultra rapid products from IGS [9], [4], one can use real-time RETICLE products from the German Space Operations Center (GSOC) / German Aerospace Center (DLR) [6]. These products have been compared in [2]. All results presented in this paper rely on RETICLE real-time satellite clocks and orbits. The RETICLE system computes clock corrections for the entire GPS constellation in real-time, currently based on a world-wide network of 37 reference stations. The estimated clocks are provided with a sampling interval of 10 seconds and a latency of 5 seconds. A more detailed description of the data-processing setup and precise orbit determination results with RETICLE products are contained in [6]. The technical aspects of using RETICLE products in real-time SF-PPP software are described in [2]. The satellite orbit position and the satellite clock error needed for PPP are extrapolated from the last nine respectively two values from the RETICLE data stream.
Next to the RETICLE products, we use predicted Global Ionospheric Maps (GIM) and predicted differential code biases (DCB) from the Center for Orbit Determination in Europe (CODE) in Bern, in order to enable real-time SF-PPP. The predicted GIMs are provided in 24 hour

batches. We use a simple linear interpolation in time, and a bi-linear interpolation in space.

Next to the abovementioned data products, models are used to account for the various error sources. These error sources can be split up into three main categories: satellite and propagation effects (as the tropospheric delay for which we use the Saastamoinen model with Ifadis mapping function), site displacements effects (as solid Earth tides) and other algorithm elements (as the relativistic effect). An extensive description of all these effects is given by [9]. The implementation of these effects in the SF-PPP software is described in [2].

The SF-PPP software at Delft University of Technology uses undifferenced single frequency pseudorange code and carrier phase observations [10]. One integral processing of these observations is carried out, with estimating carrier phase float ambiguities (as constants, as long as no cycle slips occur). The position solution is calculated on an epoch by epoch basis, i.e. truly kinematic, without any user receiver dynamics modeling (its motion can be completely free).

The stochastic model for the measurements specifies a standard deviation of 5 mm for the thermal noise and multipath effects on carrier phase, and a standard deviation ranging from 0.1 m to 1 m for the pseudorange code, depending on the actual receiver (from high-end to low-end); multipath may also include systematic effects, which are not accounted for in our model. The above values hold for a satellite in the local zenith, and elevation dependent weighting is used.

Also the inclusion of the data products is reflected in the stochastic model. Satellite orbit and clock information is said to be accurate at the few centimeter level, and an uncertainty of a few decimeters (in local zenith direction) is assigned to the ionospheric delay, which remains after applying the information from the GIM. The tropospheric delay correction using the Saastamoinen model is said to be accurate down to the one decimeter level (in local zenith direction).

Only measurements to GPS satellites are used. By default a 5 degrees satellite elevation cut-off angle is used. Statistical testing of the measurements is performed specifically on outliers and cycle slips.

DATA-COMMUNICATION FOR RT-SF-PPP

In the described experiment, measurements have been collected in the vehicle, and the needed data products have been logged – in parallel – in the office. The actual processing took place, back in the office, after the fact, but strictly re-playing the real-time situation. Only measurements up to the observation epoch are used (hence filtering, no smoothing), as well as only those data products available at the very time of the observation.

Now we provide a quick and rough calculation on the data throughput for an actual real-time implementation in the vehicle (straightforward, non-optimized). We simply represent values of all transmitted parameters with 64 bits (8 bytes – double precision (floating-point) numbers).

Corrections to the three satellite position coordinates and the satellite clock error, are sent every 5 seconds. With 32 GPS satellites, this yields about 8000 bits every 10 seconds, or about 800 bits/s. A (predicted) Global Ionospheric Map (GIM) is available each time for a 2 hour interval. The map contains Vertical Total Electron Content (VTEC) values for a worldwide grid. The VTEC map has a spatial resolution of 2.5 x 5 degrees in geographic latitude and longitude, and thereby 72 x 72 values per map (= 5184 values), roughly 330000 bits, need to be sent every 2 hours (12 maps in 24 hours). On average this amounts to just 46 bits/s. And finally the Differential Code Biases (DCBs) and Earth Rotation Parameters (ERPs) represent under 2500 bits per day. On average, the load on the data-link, including some overhead, is around one kilobit per second, or about 120 bytes/s, which is easily accommodated by today's 2.5 and 3G telecommunication infrastructure.

APPLICATION OF LANE-IDENTIFICATION

In this paper the application of SF-PPP lies in next generation car navigation, as well as in the observation and study of driver behaviour and traffic flow. The applications require the position of the car down to the lane-level. In this and the following section the application is detailed and we make a first attempt – using some simplifying assumptions – to formulate a requirement on the position error for lane identification.

Positioning of cars in a longitudinal sense, so-called car-following, and their consequences are well studied, and it has been used by car-manufacturers to develop active cruise controls, which keep car inter-distances at a constant level automatically, and also cooperative cruise controls, which coordinate longitudinal acceleration to optimize traffic flow [1].

However, lateral movements, i.e. lane changes, are an important phenomenon as well, causing a lower road capacity [8], and creating so-called stop-and-go waves [12]. Short traffic jams of stopped traffic are then 'moving' in the direction opposite to the traffic-flow. Research on this subject is relatively new, mainly due to limited possibilities to observe the lane a vehicle is driving in (and hence lane changes). For traffic control, there has been some testing of lane change assistants with simulation [11], but to the best of the authors' knowledge, no test has been performed in actual traffic. One of the issues is that behavioural research on lane changing, and lateral traffic control algorithms, require the position of the car down to the lane-level, which has not been a straightforward task up to now.

REQUIREMENTS FOR LANE-IDENTIFICATION

In the Netherlands, one lane on a motorway is 3.50 m wide, and for successful lane-identification, the cross-track (or lateral) coordinate of the position fix has to lie within this lane. Assuming the car is driving exactly in the middle of the lane, and having the antenna mounted exactly on the lengthwise center-line of the car, the probability of correct identification can be evaluated by integrating the position coordinate error probability density function (which in our case we assume to be normal) from -3.50/2 m to +3.50/2 m (i.e. a two sided

interval about zero, where zero represents the situation in which the estimated position coordinate coincides with the true position).
For a system of advanced traffic flow monitoring, which may also provide guidance instructions to enhance traffic flow, we set – as a first guess – the required probability of correct lane-identification to 95%, meaning that only 5 cars out of 100 are missed. This order of magnitude for the rate of correct identification is deemed sufficient for such a technical - non safety-of-life - system to operate successfully.
The above 95% position error requirement is applied in this paper to a single position-fix, i.e. a single epoch position solution. In practice, multiple epochs may be used, and possibly even auxiliary sensors.

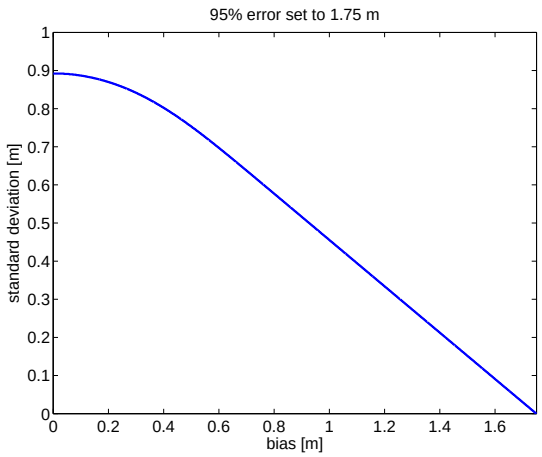

Figure 2: This curve represents a 95% position error requirement of 1.75 m, assuming a normal distribution. The horizontal axis shows the bias in the position estimator, the vertical axis shows the standard deviation of the position estimator. Below the curve lane identification is possible as the requirement is met; above the curve it is not, as the requirement is not met.

The curve in Figure 2 runs from a required standard deviation of $\sigma = 0.9$ m when there is no bias, to zero when the bias approaches the required 1.75 m. For all points on the curve, the 95% error equals 1.75 m (the graph presents a so-called iso-curve for the 95% position coordinate error about zero). This graph links – specifically for these settings – the mean and standard deviation to the 95% value, under the assumption of a normal distribution.
In discussing the results of the test, we apply the above requirement separately to both the two horizontal coordinates North and East; i.e. it has to hold for the North and for the East.

EQUIPMENT

Three classes of equipment have been used in this test. By low-end we refer to a fairly simple single frequency GPS L1 receiver, with a cost on the order of 0.1 kEuro. In the test we have used a u-blox TIM LP receiver (Evaluation Kit), 16 channels, which is – on the account of measurement accuracy – believed to be representative of a good automotive GPS-chip today. It is connected to a decent patch antenna, a Tri-M Big Brother. For the middle class we used a single frequency Septentrio AsteRx1 receiver, configured as a 16 channel GPS L1 receiver and connected to a relatively simply patch antenna, the Aero AT575; the equipment cost is here on the order of 1 kEuro. The high-end equipment consisted of a Trimble R7 12 channel dual frequency GPS receiver with a Zephyr Geodetic antenna; the equipment cost is on the order of 10 kEuro. Actually two Trimble R7 receivers were used for this experiment, of which the reason primarily lies in reconstruction of the ground truth trajectories. By default, in later sections, results of only one of them – namely the front-one - are shown (the performance of the other one is very similar). Another two Trimble R7 receivers mounted on the vehicle were used for a different experiment.
All receivers collected data at 10 Hz and were configured (to the extent possible) not to apply any measurement smoothing. And only single frequency measurements (C1 and L1) from these receivers were used for the PPP processing.
In addition to the receivers on the car, another Trimble R7 receiver was used as a reference station, a few kilometers away, located at the TU Delft GNSS observatory. This receiver was connected to an Ashtech Dorne Margolin choke-ring antenna.

EQUIPMENT INSTALLATION

Figure 3 shows the antennas of the various receivers mounted on the roof of the vehicle. All antennas were attached to a solid wooden bar, which was rigidly mounted on the vehicle. For the experiment described in this paper only the bar (in the picture) at right is used. The patch antennas for the low-end and middle class receiver are situated in the middle, and the two Zephyr Geodetic antennas of the two Trimble R7 receivers mark both ends of the wooden bar. The antennas are spaced by some 70-80 cm.

Figure 3: Antenna set-up on the roof of the test vehicle. In this paper only the antennas attached to the wooden bar at right are used. The ones at left (in the picture) are for a different experiment.

TEST SET-UP

A 5.5 km section of motorway was selected, from entrance/exit 10 (Delft Zuid) to exit/entrance 11 (Berkel en Rodenrijs / Rotterdam Airport). Next, four one-hour sessions over the day were defined, considering also satellite visibility and geometry, ionospheric activity, and traffic activity on the A13 motorway. These one-hour sessions are listed in Table 1. During these sessions, the minimum number of satellites available above a cutoff angle of 5 degrees was 9, and the maximum ranged from 11 to 13.
The 5.5 km section of motorway was driven forth and back, and during each one-hour session five loops of

driving forth and back the section were completed, yielding a total driven distance of about 57 km per session. All four sessions together gave 228 km worth of measurements, and close to 150.000 measurement epochs (at 10 Hz sampling rate).
While driving, the car changed lanes several times and driving speeds varied between 75 km/h (typically imposed by busy traffic) and 105 km/h (obeying, more or less, the legal limit of 100 km/h on this stretch of motorway). The total average speed, which includes stopping at traffic-lights at the exits and entrances, lied around 60 km/h.

Table 1: Four one-hour sessions with start and end times, on Wednesday March 16th, and Thursday March 17th, 2011. Local time is one hour ahead; thereby session 1 is just prior to afternoon rush-hour (and associated traffic jam), and session 3 is just prior to morning rush-hour.

	date (dd-mm-yyyy)	start time (UTC)	end time (UTC)
session 1	16-03-2011	13:15	14:15
session 2	16-03-2011	19:30	20:30
session 3	17-03-2011	04:45	05:40
session 4	17-03-2011	10:40	11:40

RESULTS: VISUAL IMPRESSION

In this section the Single Frequency Precise Point Positioning (SF-PPP) results are presented at a global level, primarily through visual inspection and an analysis of position solution availability. In later sections we provide a more in-depth quantitative assessment, for which we establish centimeter-level ground truth trajectories of the vehicle. Position performance will then be analysed through statistical means for both kinematic and static parts of the test.
The trajectories of the computed SF-PPP position solutions of the three receivers are overlaid on a Google™ Earth image. Visual inspection shows the general, and moreover the relative performance between the receivers. We expect that the Google™ Earth images, in an absolute sense, for this region, are geo-referenced down to the meter-level, which means that an additional shift of the images in the order of 1-2 meters in any direction is still possible. The SF-PPP position solutions are directly referenced later-on against a ground-truth in ITRF2005.

Figure 4: The test-vehicle (green van in front) on the A13 multi-lane motorway; the experiments were carried out under ordinary driving conditions, here during session 4.

Figures 5 and 6 present examples (snapshots) of trajectory overlays on Google™ Earth images, and thereby provide a first general impression of the SF-PPP positioning performance. Figures 5 and 6 present all position solutions, of all three receivers, of session 3. During this one-hour session the stretch of motorway was driven five times forth and back, so for each color there will be five dots on either side of the road. Measurements were collected at 10 Hz.
In Figures 5 and 6 the green dots represent the u-blox TIM LP receiver, the red dots the Septentrio AsteRx1 receiver and the yellow dots are the positions of the Trimble R7 receiver. Usage of different lanes can be clearly distincted from the trajectories produced by all three receivers, and in Figure 6 a change from the middle to the far left lane can be properly observed.
Availability of the SF-PPP positioning results is briefly presented in Table 2. Measurement data can be lost due to obstruction of the satellite signal. On this motorway there are tall lamp-posts every 50 meters, and on this stretch there are 11 overhead traffic portals, of which 9 'light' ones, carrying electronic signs for dynamic traffic management (see also Figure 5, and note the shadow of the portal on the road), and 2 'heavy' ones, carrying huge, traditional road and destination signs. And directly next to the motorway, there are trees and vegetation every now and then. Also large road vehicles, like trucks can cause several satellites being lost in the tracking. And finally the measurement data may be of too poor quality; it may happen that after detection of cycle slips and removal of outliers, measurements to too few satellites remain to be able to compute a position solution.

Figure 5: SF-PPP position trajectories overlaid on Google™ Earth image - results of u-blox TIM-LP receiver (green), Septentrio AsteRx1 receiver (red) and Trimble R7 receiver (yellow). The dots all show the correct lane. Note that on the North-bound stretch also the emergency lane has been used – the dynamic traffic management system allows to do so during rush hours (as was session 3, see also Figure 1).

Figure 6: SF-PPP position trajectories overlaid on Google™ Earth image - results of u-blox TIM-LP receiver (green), Septentrio AsteRx1 receiver (red) and Trimble R7 receiver (yellow). The dots all show the correct lane. On the North-bound stretch this figure demonstrates a lane-change, to the far most left lane.

Availability of the SF-PPP solution is very good in all sessions with all receivers. The availability is always larger than 99%.

Table 2: Availability of SF-PPP results of the three receivers during the four sessions as a percentage of the total number of (theoretically) available epochs (at a 10 Hz rate).

receiver	session 1 (%)	session 2 (%)	session 3 (%)	session 4 (%)
u-blox TIM LP	99.73	99.75	99.72	99.73
Septentrio AsteRx1	99.11	100.00	99.70	99.81
Trimble R7	99.23	99.81	99.26	99.43

GROUND-TRUTH TRAJECTORIES

In this section we spend a few words on the ground-truth trajectories, that are produced and used to assess SF-PPP positioning performance in a quantitative sense, for both kinematic and static parts of the test.

The high-end receivers were used to compute accurate (cm-level) ground-truth trajectories for themselves, and also to reconstruct those for the low-end and middle-class receivers. The ground truth trajectories were computed, using Trimble Geomatics Office (TGO) software, with dual frequency differential carrier-phase GPS to a nearby reference station, namely a station at TU Delft´s GNSS observatory (located at the Netherlands Metrology Institute (NMi)), with accurately known position coordinates in the International Terrestrial Reference Frame (ITRF2005). The baseline length ranged from just half a kilometer to some four kilometers.

As shown in Figure 3, all antennas were mounted (without adapters) on the center line of the same wooden bar, and this allowed for an easy reconstruction of the ground truth trajectory, also of the low-end and middle class receiver, as distances along the (straight line) bar had been measured between the antennas. Thereby, slightly different sampling times of the receivers have been neglected (the receivers in this test keep their time within 1 millisecond to the GPS time). With a maximum driving speed of 30 m/s, the effect is a few cm at maximum, which is neglected, considering the expected decimeter positioning accuracy of SF-PPP.

As a result of this section we do have accurate, centimeter-level, ground-truth trajectories available for all of the receivers; in this contribution we specifically analyse a stretch of the kinematic part (one North-bound drive from entrance 11 to exit 10 on the motorway, worth of about 4 minutes of data), for each of the four sessions, and a static part at entrance 10 of the motorway, worth of 5 minutes of data, for sessions 2 and 3.

The position errors analysed in the next few sections are obtained by differencing the SF-PPP results with the ground truth trajectories. Position accuracy is then presented in terms of three statistics for each of the three coordinate components, North (N), East (E), and Up (U): first the mean of the error (estimated minus truth), secondly the empirical standard deviation (std) of the error about the mean, and finally the 95 percentile of the error (about zero), generally referred to as the 95% (percent) error.

KINEMATIC RESULTS

From each session one ‘run’ was selected in North-bound direction for detailed analysis (entering the motorway at entrance 11, and leaving it at exit 10). The results in terms of mean, standard deviation (std) and 95% of the SF-PPP position errors are given in Tables 3, 4 and 5, for respectively the (low-end) u-blox TIM LP receiver, the (middle class) Septentrio AsteRx1 receiver (with patch antenna), and the (high-end) Trimble R7 receiver.

Once more it is stated that these SF-PPP results are truly kinematic; no modeling of the vehicle dynamics or whatsoever is included. The measurements are processed recursively [10], epoch-after-epoch, and receiver position coordinates are estimated together with the receiver clock error, each epoch anew, and only the carrier phase ambiguities are propagated – as constants – from one epoch to the next.

There does not seem to be much difference in performance between the middle class (with patch antenna) and high-end receiver. The u-blox TIM LP SF-PPP results are generally a factor 2-3 worse when looking at the 95% figures, in particular in the Up-component. All

receivers seem to meet the 1.75 m (95%) requirement on the horizontal coordinates.

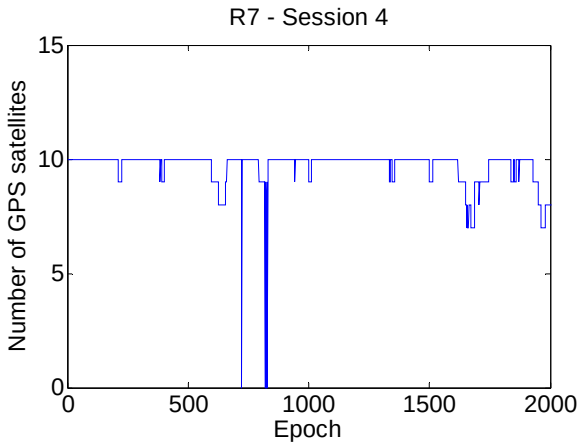

Figure 7: Number of GPS satellites used in PPP solution (during one North bound 'run'); zero satellites corresponds to no solution available, either due to too few satellites tracked by the receiver, or too few satellites remaining after statistical testing of the measurements.

On the selected North-bound stretch – over all four sessions – there are only little differences in the number of GPS satellites used in the position solution between the receivers; generally there is up to only one satellite of a difference among them. The number of satellites used in the position solution generally varies from 8 to 11. Figure 7 shows the number of GPS satellites used in the position solution for the R7 receiver, as a function of time (measurements were collected at 10 Hz), where time zero corresponds to the start of the selected North-bound 'run'. Whenever the position solution is unavailable, the number of satellites is set to zero, and these epochs are counted to determine the availability as shown in Table 2. On this stretch there are 9 'light' overhead traffic portals, and 2 'heavy' ones.

To investigate the possible influence of ionospheric activity, four sessions were performed: session 1 in the afternoon, session 2 in the evening, session 3 during late night and session 4 in the morning respectively. The daily local peak of the ionospheric zenith delay is known to occur in the afternoon. For this analysis we will make use of the R7 receiver which is expected to be least sensitive to multipath. The influence of the ionosphere will be mainly visible in the Up-component, due to the GPS satellite geometry and the fact that the ionosphere will cause a delay on the GPS signals. In Table 5, we observe that the 95% errors are lowest for the Up-components during evening and morning (sessions 2 and 3) compared to the sessions during mid-day (sessions 1 and 4), and the same holds for the mean and standard deviation, but differences are not very distinct.

Table 3: SF-PPP results expressed in local North, East, and Up components for selected North-bound kinematic part of all four sessions, for u-blox TIM LP receiver. Given are mean, standard deviation (std) and 95% errors.

	mean [m]			std [m]			95 % [m]		
	N	E	U	N	E	U	N	E	U
u-blox TIM LP (number of epochs)									
session 1 (1835)	0.25	-0.79	0.21	0.38	0.25	1.06	0.96	1.12	2.03
session 2 (1795)	-0.82	0.30	-0.36	0.29	0.33	1.60	1.20	0.67	2.36
session 3 (1842)	0.60	0.00	-1.36	0.42	0.31	0.78	1.03	0.57	2.05
session 4 (2006)	0.38	-0.20	1.12	0.40	0.31	1.02	0.96	0.89	2.12

Table 4: SF-PPP results expressed in local North, East, and Up components for selected North-bound kinematic part of all four sessions, for Septentrio AsteRx1 receiver. Given are mean, standard deviation (std) and 95% errors.

	mean [m]			std [m]			95 % [m]		
	N	E	U	N	E	U	N	E	U
Septentrio AsteRx1 (number of epochs)									
session 1 (1841)	0.11	-0.50	-0.03	0.08	0.12	0.13	0.30	0.64	0.24
session 2 (1801)	-0.72	0.49	-0.51	0.25	0.20	0.18	1.08	0.84	0.84
session 3 (1831)	-0.05	-0.13	0.24	0.11	0.18	0.21	0.21	0.32	0.52
session 4 (2011)	0.03	0.05	0.21	0.17	0.10	0.14	0.27	0.20	0.55

Table 5: SF-PPP results expressed in local North, East, and Up components for selected North-bound kinematic part of all four sessions, for Trimble R7 receiver. Given are mean, standard deviation (std) and 95% errors.

	mean [m]			std [m]			95 % [m]		
	N	E	U	N	E	U	N	E	U
Trimble R7 (number of epochs)									
session 1 (1820)	0.20	-0.05	0.41	0.10	0.10	0.25	0.37	0.23	0.88
session 2 (1795)	-0.48	0.18	-0.19	0.10	0.10	0.19	0.64	0.34	0.50
session 3 (1846)	0.02	0.11	0.29	0.12	0.11	0.19	0.23	0.27	0.59
session 4 (2005)	-0.41	0.15	0.45	0.12	0.08	0.22	0.61	0.28	0.80

STATIC RESULTS

Before starting a session, the car was parked alongside the road for five minutes to obtain a static solution for all receivers. Results of two of these static parts, of sessions 2 and 3, are presented in Tables 6, 7 and 8. For a two dimensional graphical overview of the SF-PPP results versus the ground truth, a scatter plot is given in Figure 8. In this figure we have plotted the horizontal coordinates of the solutions for six receivers: the four Trimble receivers coined R7A, R7B, R76 and R77 at the ends of both wooden bars (see Figure 3), the Septentrio AsteRx1 and the u-blox TIMLP receivers placed on the same bar as, and in between, the R7A and R7B receivers. The black dots indicate the ground truth positions of the receivers, and R7B is selected as the centre of the figure. The left hand side is the static part of session 2 and the right hand side of session 3. For the Trimble receivers we observe a cloud of solutions centered more or less around the ground truth of the receiver, whereas the solutions for the AsteRx1 and the TIMLP are not so much a cloud and are further away from the ground truth.

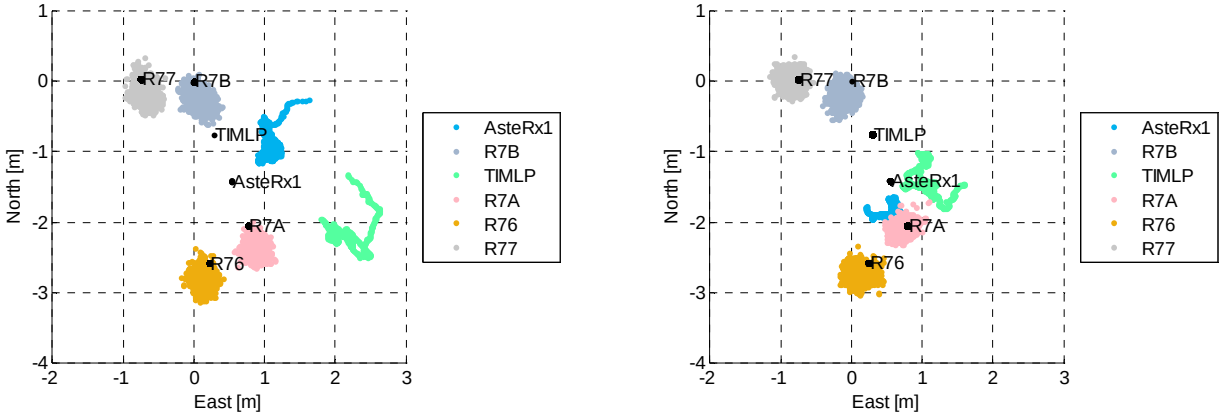

Figure 8: Static SF-PPP results for all receivers on the car, together with the ground truth positions (indicated by the black dots), for 5 minutes static part in session 2 (left) and session 3 (right). Horizontal positions in local East and North; the car is heading to the local South-East.

Table 6: SF-PPP results expressed in local North, East, and Up components for two static parts in sessions 2 and 3, for u-blox TIM LP receiver. Given are mean, standard deviation (std) and 95% errors.

	mean [m]			std [m]			95 % [m]		
	N	E	U	N	E	U	N	E	U
u-blox TIM LP									
session 2	-1.41	1.82	3.03	0.17	0.21	0.45	1.70	2.23	3.68
session 3	-0.67	0.73	1.02	0.19	0.16	0.53	0.91	1.01	1.78

Table 7: SF-PPP results expressed in local North, East, and Up components for two static parts in sessions 2 and 3, for Septentrio AsteRx1 receiver. Given are mean, standard deviation (std) and 95% errors.

	mean [m]			std [m]			95 % [m]		
	N	E	U	N	E	U	N	E	U
Septentrio AsteRx1									
session 2	0.51	0.54	0.09	0.10	0.08	0.29	0.81	0.67	0.69
session 3	-0.45	0.06	-1.69	0.11	0.12	0.22	0.64	0.27	1.96

Table 8: SF-PPP results expressed in local North, East, and Up components for two static parts in sessions 2 and 3, for Trimble R7 receiver. Given are mean, standard deviation (std) and 95% errors.

	mean [m]			std [m]			95 % [m]		
	N	E	U	N	E	U	N	E	U
Trimble R7									
session 2	-0.32	0.11	0.09	0.10	0.08	0.09	0.47	0.24	0.37
session 3	-0.05	-0.09	-0.52	0.08	0.08	0.16	0.17	0.22	0.79

The two five minutes static parts gave moderately sized biases for the high-end reference receivers with surveying grade antennas (namely the Trimble Zephyr Geodetic), but clearly larger biases for the other two receivers with patch antennas. The most likely explanation for these biases is multipath on the pseudorange code observations and in order to analyze this hypothesis, we have calculated the single difference residuals on the baselines between

1) the two Zephyr Geodetic antennas connected to the Trimble R7 receivers at both ends of the wooden bar, and

2) between one of the Zephyr Geodetic antennas connected to the R7 receiver and the patch antenna connected to the u-blox TIM LP receiver.

The single difference residuals of the epoch by epoch solutions are shown in Figure 9 as an example for the pseudo range code measurements collected from the GPS satellite with PRN number 18. As is shown in Figure 10, the satellite is at about 28 degrees above the horizon at the time of the static test, and descending. The residuals are obtained through applying the baseline for this static test as a known vector (constrained). The left hand side of the figure shows the residuals on the baseline formed by the two Trimble receivers, on the right hand side we show the baseline between the Trimble and u-blox receiver with patch antenna. The measurements were collected simultaneously.

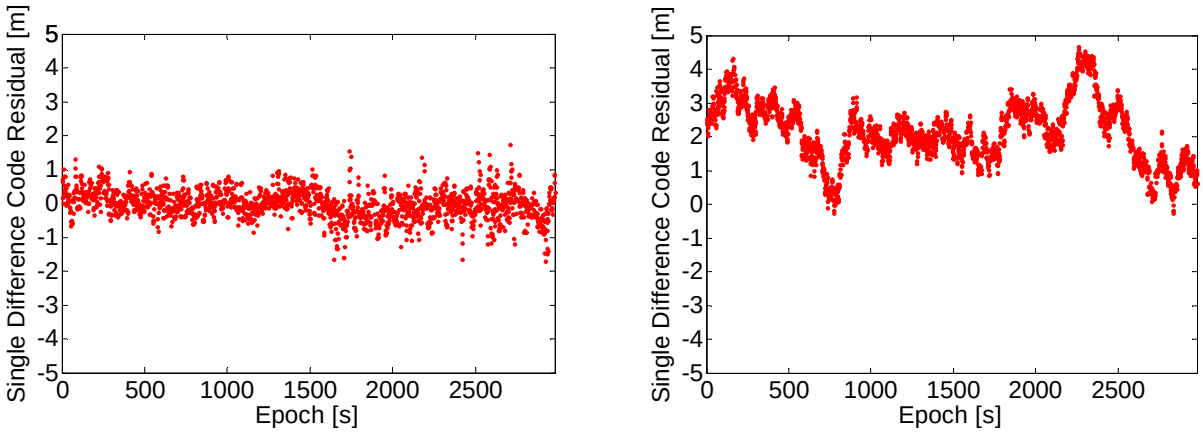

Figure 9: Single difference residuals of pseudorange measurements to satellite PRN18 for the baseline between the two Zephyr Geodetic antennas connected to Trimble R7 receivers at both ends of the wooden bar (left), and one of the Zephyr Geodetic antennas (Trimble R7) and the u-blox TIM LP with patch antenna (right); static part of session 2.

On the left hand side the residuals show a more or less a zero-mean random behaviour, where on the right side there is a clearn offset of a few meters plus time varying errors with a period of tens of seconds. This analysis strongly indicates that the multipath hypothesis is likely (reflection by the vehicle's roof and/or the road surface) as the residuals on the second baseline show typical characteristics of a signal affected by multipath.

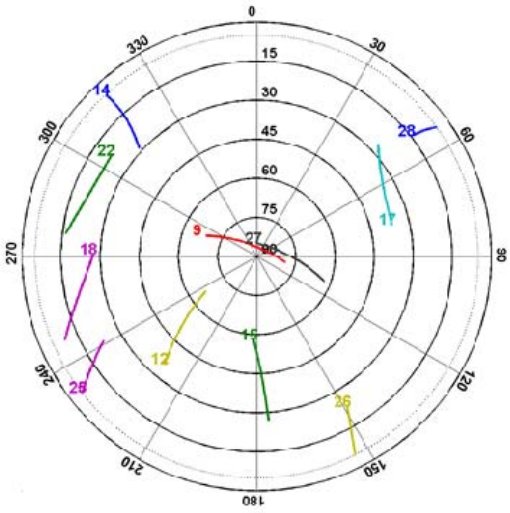

Figure 10: Skyplot for session 2 on March 16th, 2011, from 19:30 to 20:30 (UTC)

Both the low-end and middle class receiver use a patch antenna, but nevertheless differences can still be observed in the results in Tables 6 and 7 between the u-blox TIM LP and the Septentrio AsteRx1 receiver. The u-blox likely uses (close to) the minimum bandwidth (2 MHz) for the GPS CA-code signal, whereas the Septentrio receiver uses a much wider band. The latter translates into capabilities of multipath mitigation by receiver signal processing (hence, smaller biases compared to the u-blox), and into higher measurement precision (smaller standard deviation values).

The low-end receiver does not always meet the 1.75 m requirement in these static parts. The measurement precision does not seem to be the limiting factor (standard deviations of the horizontal coordinates lie in the order of only 0.20 m), but multipath seems to be the hurdle, with the reason lying in the patch antenna, in combination with limited signal processing capabilities in the receiver due to the small signal bandwidth used.

Compared with the kinematic results in Tables 3, 4 and 5, the bias values seem to be slightly larger with the static results (Tables 6, 7 and 8). Under kinematic circumstances, i.e. driving a vehicle at 70-100 km/h, the environment of the receiver antenna is changing pretty much, and thereby multipath effects tend to be more randomly.

CONCLUSIONS

The position accuracy achieved with the low-cost receiver during the trial is about 0.30 – 0.40 m and 0.50 – 1.00 m generally, in terms of standard deviation for the horizontal and vertical coordinates respectively. A 95% position error of less than 1.75 m is met in most cases for the horizontal coordinates – a lane on a motorway in the Netherlands is 3.50 m wide. These results show that Real-Time Single Frequency – Precise Point Positioning (RT-SF-PPP) can be used for lane identification, when relying

on fairly cheap equipment. The kinematic test showed a SF-PPP solution availability of larger than 99%.

The paper has also outlined the requirements on data communication for RT-SF-PPP. In brief the required data rate to the vehicle on average is around 1 kbit/s, which is easily accommodated by today´s 2.5 and 3G telecommunication infrastructure.

ACKNOWLEDGMENTS

The continued provision of RETICLE products by André Hauschild at DLR (German Aerospace Center) is acknowledged. The u-blox TIM LP receiver was kindly made available for the experiment by Mr. Sam Storm van Leeuwen.

REFERENCES

[1] van Arem, B., C.J.G. van Driel, and R. Visser (2006). The Impact of Cooperative Adaptive Cruise Control on Traffic-Flow Characteristics. IEEE Transactions on Intelligent Transportation Systems. Vol. 7, No. 4. pp. 429-436.

[2] van Bree, R.J.P., C.C.J.M. Tiberius, and A. Hauschild (2009). Real Time Satellite Clocks in Single Frequency Precise Point Positioning. Proceedings ION-GNSS-2009. Sept. 22-25. Savannah, Georgia, USA. pp. 2400-2414.

[3] van Bree, R.J.P., C.C.J.M. Tiberius (2011). Real Time Single Frequency Precise Point Positioning - accuracy assessment. GPS Solutions. DOI 10.1007/s10291-011-0228-6.

[4] Dow, J.M., R.E. Neilan, and G. Gendt (2005). The International GPS Service (IGS): Celebrating the 10th Anniversary and Looking to the Next Decade. Adv. Space Res. 36 Vol. 36, No. 3, pp. 320-326.

[5] Gao, Y., Y. Zhang, and K. Chen (2006). Development of a real-time single-frequency Precise Point Positioning system and test results. Proceedings of ION GNSS 2006. Sept. 26-29. Fort Worth, Texas. pp. 2297-2303.

[6] Hauschild, A., O. Montenbruck (2008). Real-time Clock Estimation for Precise Orbit Determination of LEO-Satellites. Proceedings of the ION GNSS Meeting 2008. Sept. 16-19. Savannah, Georgia, USA. pp. 581-589.

[7] Héroux, P., and J. Kouba (1995). GPS Precise Point Positioning with a Difference. Geomatics'95. June 13-15., Ottawa, Ontario, Canada.

[8] Jin, W. L. (2010). Macroscopic characteristics of lane-changing traffic. 89th Annual Meeting of the Transportation Research Board. Washington DC. January 10-14.

[9] Kouba, J., (2009). A Guide to using international GPS service (IGS) products. Online publication at IGS website http://igscb.jpl.nasa.gov/components/usage.html

[10] Le, A.Q., and C.C.J.M Tiberius (2007). Single-frequency precise point positioning with optimal filtering. GPS Solutions. Vol. 11, No.1. pp. 61-69.

[11] Pueboobpaphan, R., F. Liu, and B. van Arem (2010). The impacts of a communication based merging assistant on traffic flows of manual and equipped vehicles at an on-ramp using traffic flow simulation. 13th International IEEE Annual Conference on Intelligent Transportation Systems (ITSC). Madeira Island, Portugal. September 19-22. pp. 1468-1473.

[12] Zheng, Z., S. Ahn, D. Chen, and J. Laval (2011). Freeway traffic oscillations: microscopic analysis of formations and propagations using wavelet transform. Procedia Social and Behavioral Sciences. Vol. 17. International Symposium on Transportation and Traffic Theory. pp. 717–731.

[13] Øvstedal, O. (2002). Absolute positioning with single frequency GPS receivers. GPS Solutions. Vol. 5, No.4. pp. 33-44.